# SPARSE CENTROID-ENCODER: A NONLINEAR MODEL FOR FEATURE SELECTION

# Tomojit Ghosh

Department of Computer Science Colorado State University Fort Collins, CO 80523-1873 tomojit.ghosh@colostate.edu

#### Michael Kirby

Department of Mathematics Colorado State University Fort Collins, CO 80523-1873 Kirby@math.colostate.edu

February 1, 2022

#### **ABSTRACT**

We develop a sparse optimization problem for the determination of the total set of features that discriminate two or more classes. This is a sparse implementation of the centroid-encoder for nonlinear data reduction and visualization called Sparse Centroid-Encoder (SCE). We also provide a feature selection framework that first ranks each feature by its occurrence, and the optimal number of features is chosen using a validation set. The algorithm is applied to a wide variety of data sets including, single-cell biological data, high dimensional infectious disease data, hyperspectral data, image data, and speech data. We compared our method to various state-of-the-art feature selection techniques, including two neural network-based models (DFS, and LassoNet), Sparse SVM, and Random Forest. We empirically showed that SCE features produced better classification accuracy on the unseen test data, often with fewer features.

### 1 Introduction

Technological advancement has made high-dimensional data readily available. For example, in bioinformatics, the researchers seek to understand the gene expression level with microarray or next-generation sequencing techniques where each point consists of over 50,000 measurements [1, 2, 3, 4]. The abundance of features demands the development of feature selection algorithms to improve a Machine Learning task, e.g., classification. Another important aspect of feature selection is knowledge discovery from data. Which biomarkers are important to characterize a biological process, e.g., the immune response to infection by respiratory viruses such as influenza [5]? Additional benefits of feature selection include improved visualization and understanding of data, reducing storage requirements, and faster algorithm training times.

Feature selection can be accomplished in various ways that can be broadly categorized into the filter, wrapper, and embedded methods. In a filter method, each variable is ordered based on a score. After that, a threshold is used to select the relevant features [6]. Variables are usually ranked using correlation [7, 8], and mutual information [9, 10]. In contrast, a wrapper method uses a model and determines the importance of a feature or a group of features by the generalization performance of the predetermined model [11, 12]. Since evaluating every possible combination of features becomes an NP-hard problem, heuristics are used to find a subset of features. Wrapper methods are computationally intensive for larger data sets, in which case search techniques like Genetic Algorithm (GA) [13] or Particle Swarm Optimization (PSO) [14] are used. In embedded methods, feature selection criteria are incorporated within the model, i.e., the variables are picked during the training process [15]. Iterative Feature Removal (IFR) uses the absolute weight of a Sparse SVM model as a criterion to extract features from the high dimensional biological data set [5].

This paper proposes a new embedded variable selection approach called Sparse Centroid-Encoder (SCE) to extract features when class labels are available. Our method extends the Centroid-Encoder model [16, 17], where we applied a  $l_1$  penalty to a sparsity promoting layer between the input and the first hidden layer. We evaluate this Sparse

Centroid-Encoder on diverse data sets and show that the selected features produce better generalization than other state-of-the-art techniques. Our results showed that SCE picked fewer features to obtain high classification accuracy. As a feature selection tool, SCE uses a single model for the multi-class problem without the need to create multiple one-against-one binary models typical of linear methods, e.g., Lasso [18], or Sparse SVM [19]. Although SCE can be used both in binary and multi-class problems, we focused on the multi-class feature selection problem in this paper. The work of [20] also uses a similar sparse layer between the input and the first hidden with an Elastic net penalty while minimizing the classification error with a softmax layer. The authors used Theano's symbolic differentiation [21] to impose sparsity. In contrast, our approach minimizes the centroid-encoder loss with an explicit differentiation of the  $l_1$  function using the sub-gradient. Unlike DFS, our model can capture the intra-class variability by using multiple centroids per class. This property is beneficial for multi-modal data sets.

The article is organized as follows: In Section 2 we present the Sparse Centroid-Encoder algorithm. In Section 3 we apply SCE to a range of bench-marking data sets taken from the literature. In Section 4, we review related work, for both linear and non-linear feature selection. In Section 5, we present our discussion and conclusion.

# 2 Sparse Centroid-Encoder

Centroid-encoder (CE) neural networks are the starting point of our approach [17, 16, 22]. We present a brief overview of CEs and demonstrate how they can be extended to perform non-linear feature selection.

### 2.1 Centroid-encoder

The CE neural network is a variation of an autoencoder and can be used for both visualization and classification tasks. Consider a data set with N samples and M classes. The classes denoted  $C_j, j=1,\ldots,M$  where the indices of the data associated with class  $C_j$  are denoted  $I_j$ . We define centroid of each class as  $c_j = \frac{1}{|C_j|} \sum_{i \in I_j} x^i$  where  $|C_j|$  is the cardinality of class  $C_j$ . Unlike autoencoder, which maps each point  $x^i$  to itself, the CE maps each point  $x^i$  to its class centroid  $c_j$  by minimizing the following cost function over the parameter set  $\theta$ :

$$\mathcal{L}_{ce}(\theta) = \frac{1}{2N} \sum_{j=1}^{M} \sum_{i \in I_j} \|c_j - f(x^i; \theta)\|_2^2$$
(1)

The mapping f is composed of a dimension reducing mapping g (encoder) followed by a dimension increasing reconstruction mapping h (decoder). The output of the encoder is used as a supervised visualization tool [17, 16], and attaching another layer to map to the one-hot encoded labels performs robust classification [22].

# 2.2 Sparse Centroid-encoder for feature selection

The Sparse Centroid-encoder (SCE) is a modification to the centroid-encoder architecture as shown in Figure 1. Unlike centroid-encoder, we haven't used a bottleneck architecture as visualization is not our aim here. The input layer is connected to the first hidden layer via the sparsity promoting layer (SPL). Each node of the input layer has a weighted one-to-one connection to each node of the SPL. The number of nodes in these two layer are the same. The nodes in SPL don't have any bias or non-linearity. The SPL is fully connected to the first hidden layer, therefore the weighted input from the SPL will be passed to the hidden layer in the same way that of a standard feed forward network. During training, a  $l_1$  penalty will be applied to the weights connecting the input layer and SPL layer. The sparsity promoting  $l_1$  penalty will drive most of the weights to near zero and the corresponding input nodes/features can be discarded. Therefore, the purpose of the SPL is to select important features from the original input. Note we only apply the  $l_1$  penalty to the parameters of the SPL.

Denote  $\theta_{spl}$  to be the parameters (weights) of the SPL and  $\theta$  to be the parameters of the rest of the network. The cost function of sparse centroid-encoder is given by

$$\mathcal{L}_{sce}(\theta) = \frac{1}{2N} \sum_{j=1}^{M} \sum_{i \in I_j} \|c_j - f(x^i; \theta))\|_2^2 + \lambda \|\theta_{spl}\|_1$$
 (2)

where  $\lambda$  is the hyper-parameter which controls the sparsity. A larger value of  $\lambda$  will promote higher sparsity resulting more near-zero weights in SPL. In other words,  $\lambda$  is a knob that controls the number of features selected from the input data.

Like centroid-encoder, we trained sparse centroid-encoder using error backpropagation, which requires the gradient of the cost function of Equation 2. As  $l_1$  function is not differentiable at 0, we implement this term using the sub-gradient.

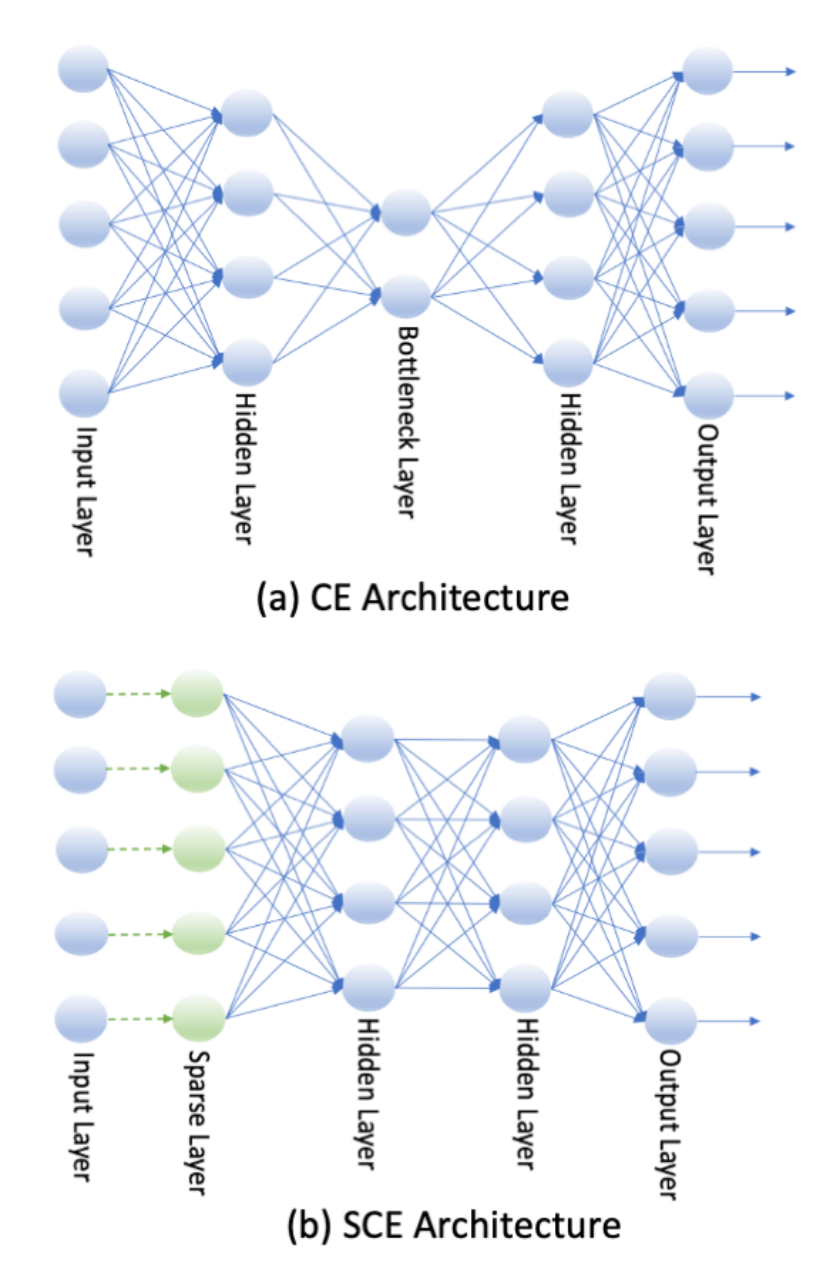


Figure 1: The architecture of Centroid-encoder and Sparse Centroid-encoder. Notice the Centroid-encoder uses a bottleneck architecture which is helpful for visualization. In contrast, the Sparse Centroid-encoder doesn't use any bottleneck architecture; instead, it employs a sparse layer between the input and the first hidden layer to promote feature sparsity.

## 2.3 Empirical Analysis of SCE

In this section we present an empirical analysis of our model. The results of feature selection for the digits 5 and 6 from the MNIST set are displayed in Figure 2. In panel (a), we compare the two terms that contribute to Equation 2, i.e., the centroid-encoder and  $l_1$  costs, weighted with different values of  $\lambda$ . As expected, we observe that the CE cost monotonically decreases with  $\lambda$ , while the  $l_1$  cost increases as  $\lambda$  decreases. For larger values of  $\lambda$ , the model focuses more on minimizing the  $l_1$ -norm of the sparse layer, which results in smaller values. In contrast, the model pays more attention to minimizing the CE cost for small  $\lambda$ s; hence we notice smaller CE cost and higher  $l_1$  cost.

Panel (b) of Figure 2 shows the accuracy on a validation set as a function nine different values of  $\lambda$ ; the validation accuracy reached its peak for  $\lambda = 0.001$ . In panels (c) and (d), we plotted the magnitude of the feature weights of

the sparse layer in descending order. The sharp decrease in the magnitude of the weights demonstrates the promotion of sparsity by SCE. The model effectively ignores features by setting their weight to approximately zero. Notice the model produced a sparser solution for  $\lambda=0.1$ , selecting only 32 features compared to 122 chosen variables for  $\lambda=0.001$ . Figure 3 shows the position of the selected features, i.e., pixels, on the digits 5 and 6. The intensity of the color represents the feature's importance. Dark blue signifies a higher absolute value of the weight, whereas light blue means a smaller absolute weight.

Our last analysis shows how SCE extracts informative features from a multi-modal dataset, i.e., data sets whose classes appear to have multiple clusters. In this case, one center per class may not be optimal, e.g., ISOLET data. To this end, we trained SCE using a different number of centers per class where the centers were determined using standard k-Means algorithm [23, 24]. After the feature selection, we calculated the validation accuracy and plotted it against the number of centers per class in Figure 4. The validation accuracy jumped significantly from one center to two centers per class. The increased accuracy indicates that the speech classes are multi-modal, further validated by the two-dimensional PCA plot of the three classes shown in panel (b)-(d).

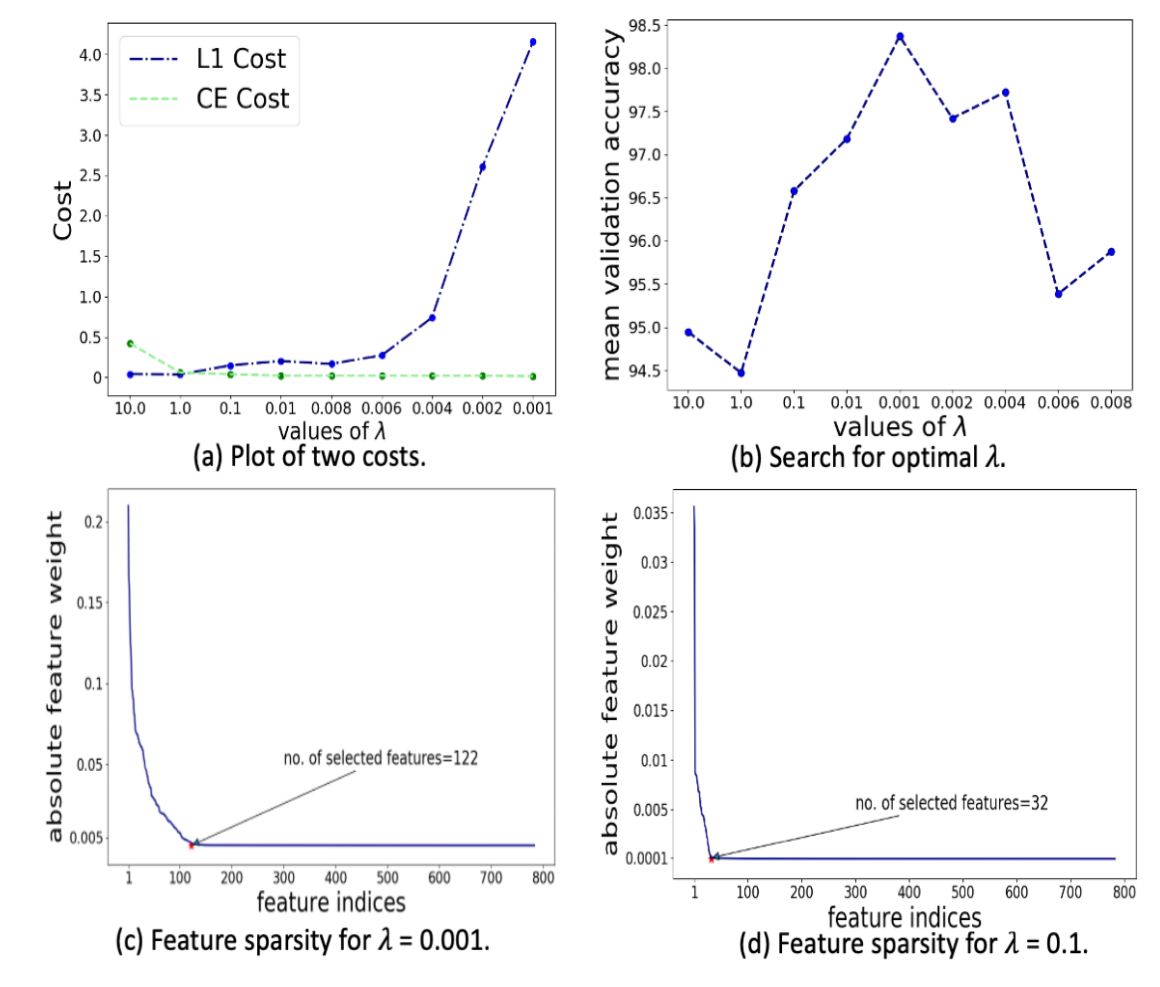


Figure 2: Analysis of Sparse Centroid-encoder. (a) Change of the two costs over  $\lambda$ . (b) Change of validation accuracy over  $\lambda$ . (c) Sparsity plot of the weight of  $W_{SPL}$  for  $\lambda=0.001$ . (d) Same as (c) but  $\lambda=0.1$ .

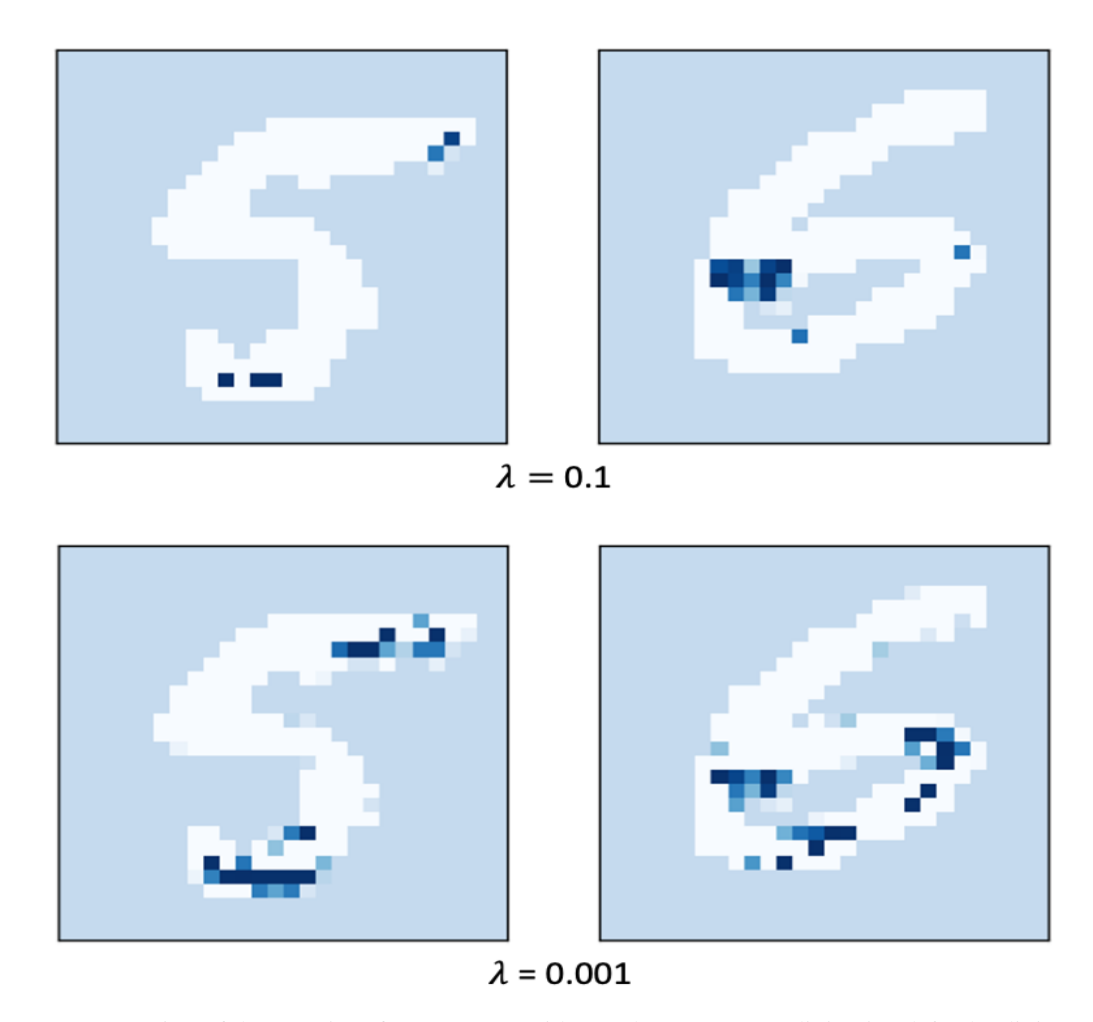


Figure 3: Demonstration of the sparsity of Sparse Centroid-encoder on MNIST digits 5 and 6. The digits are shown in white, and the selected pixels are marked using blue—the darkness of blue indicates the relative importance of the pixel to distinguish the two digits. We showed the selected pixels for two choices of  $\lambda$ . Notice that for  $\lambda=0.1$ , the model chose the lesser number of features, whereas it picked more pixels for  $\lambda=0.001$ .  $\lambda$  is the nob which controls the sparsity of the model.

# 2.4 Feature Selection Workflow Using Sparse Centroid-Encoder

By design, sparse methods identify a small number of features that accomplish a classification task. If one is interested in *all* the discriminatory features that can be used to separate multiple classes, then one can repeat the process of removing good features. This section describes how sparse centroid-encoder (SCE) can be used iteratively to extract all discriminatory features from a data set; see [5] for an application of this approach to sparse support vector machines.

SCE is a model based on neural network architecture; hence, it's a non-convex optimization. As a result, multiple runs will produce different solutions, i.e., different feature sets on the same training set. These features may not be optimal given an unseen test set. To find out the robust features from a training set, we resort to frequency-based feature pruning. In this strategy, first, we divide the entire training set into k folds. On each of these folds, we ran the SCE and picked the top N (user select) number of features. We repeat the process T times to get  $k \times T$  feature sets. Then we count the number of occurrences of each feature and call this number the frequency of a feature. We ordered the features based on the frequency and picked the optimum number from a validation set. We present the feature selection work flow in Figure 5. We trained SCE using Scaled Conjugate Gradient Descent [25]. The architectural details are kept in Appendices.

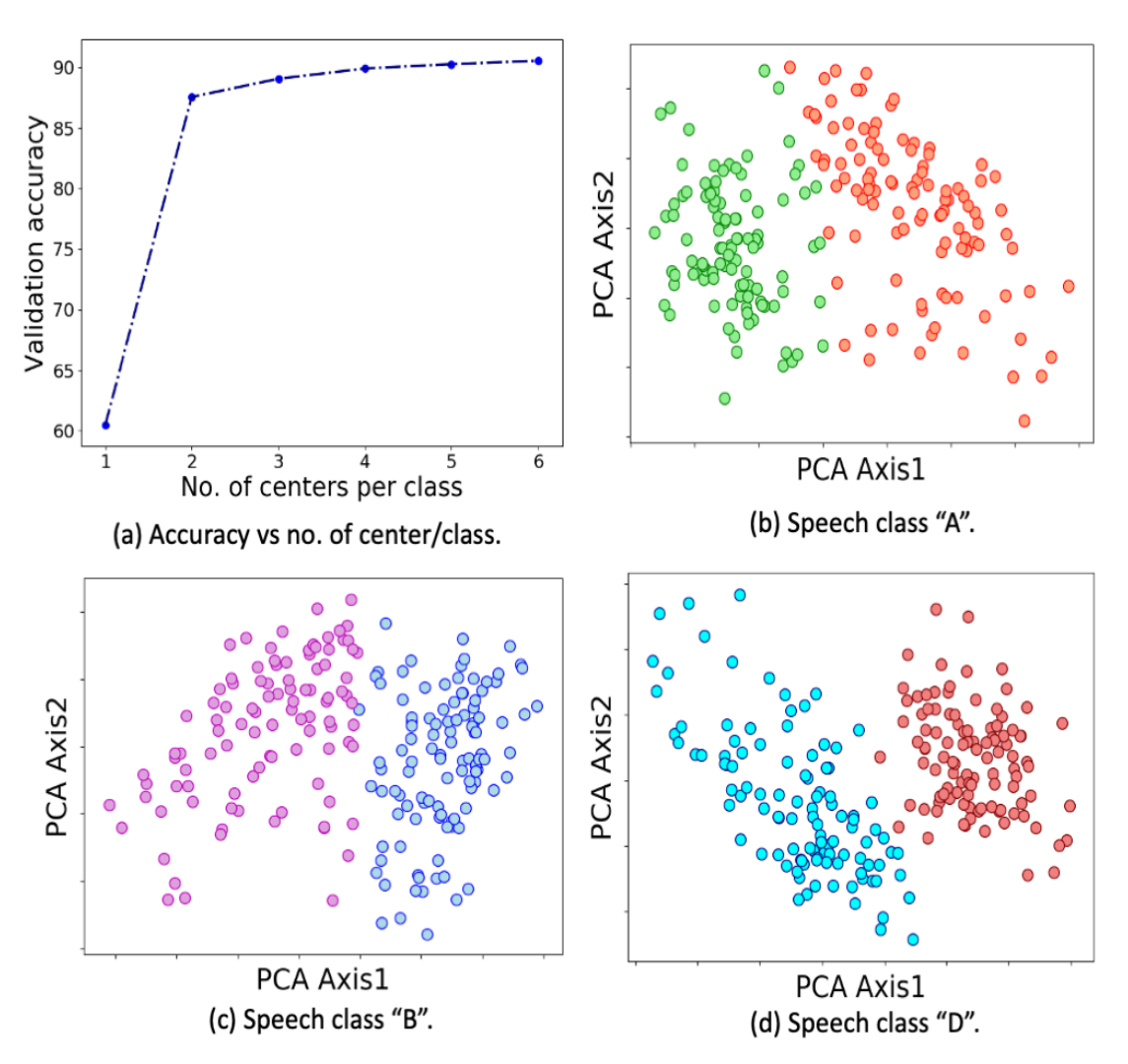


Figure 4: Sparse Centroid-encoder for multi-modal data set. Panel (a) shows the increase in validation accuracy over the number of centroids per class. Panel (b)-(d) shows the two-dimensional PCA plot of the three speech classes.

# 3 Experimental Results

Here we present a range of comparative benchmarking experiments on a variety of data sets and feature selection models. We used nine data sets from a variety of domains to run experiments.

# 3.1 Experimental Details

We did bench-marking experiments to compare the sparse centroid-encoder with other state-of-the-art feature selection methods. To make the evaluation objective, we compared the classification accuracy on the unseen data using the selected features of different models. All experiments share the following workflow:

- SCE is used to select an optimal number of features on the training samples. We chose the  $l_1$  penalty from a set of values 0.1, 0.01, 0.002, 0.004, 0.006, 0.008, 0.001, 0.0001 using a validation set.
- Build K classification models with these features on the training set. We used centroid-encoder and one hidden layer artificial neural networks as the classification model [22].
- ullet Compute the accuracy on the sequestered test set using the K trained models and report the mean accuracy with standard deviation.

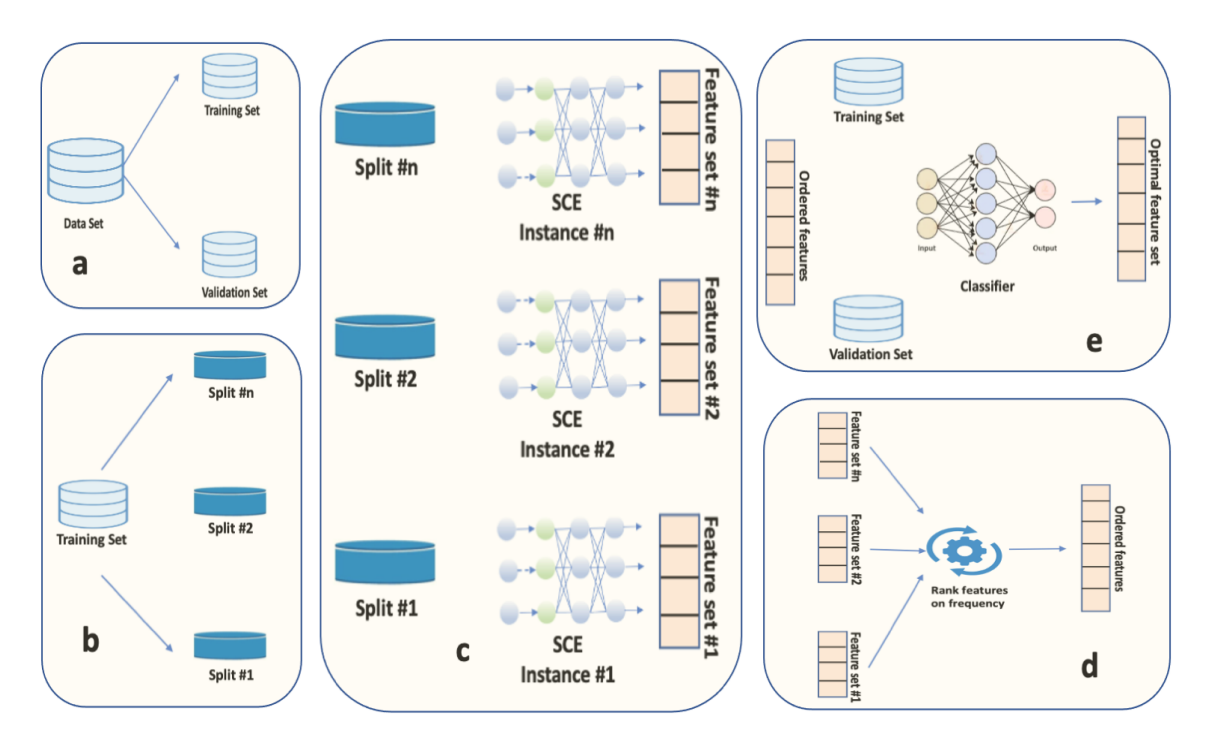


Figure 5: Feature selection workflow using Sparse Centroid-encoder. **a** First, the data set has been partitioned into training and validation. **b** We further partitioned the training set into n splits. **c** On each of the training splits, we ran Sparse Centroid-encoder to get n feature sets. **d** We calculated the occurrence of each feature among the n sets and called it the frequency of the feature. We ranked features from high to a low frequency to get an ordered set. **e** At last, we picked the optimum number of features using a validation set.

# 3.2 Quantitative and Qualitative Analysis

Now we present the results from a comprehensive analysis across nine data sets.

# 3.2.1 Comparison with LassoNet on UCI data sets

In our first set of experiments, we compared SCE with LassoNet [26] on six publicly data sets taken from different domains, including image (MNIST, Fashion MNIST, COIL-20), speech (ISOLET), activity recognition (Human Activity Recognition Using Smartphones), and a biological data set (Mice Protein data). These data sets have been used in the literature for benchmarking [26, 27]. Following the experimental protocol of Lemhadri et al., we randomly partitioned each data set into a 70:10:20 split of training, validation, and test set. We normalized the training partition by subtracting the mean and dividing each feature by its corresponding standard deviation. We used the mean and standard deviation of the training to standardize the test samples. We used the training set for feature selection and the validation set for hyperparameter tuning. After the feature selection, we used a one hidden layer neural network classifier to predict the class label on the test set. We ran the classifier ten times (K=10) and presented the mean accuracy with standard deviation in Table 1. Apart from showing the accuracy with top-50 features, we also give classification results with an optimum number of features selected using the validation set.

As we can see from Table 1, the features of the Sparse Centroid-encoder produce better classification accuracy than LassoNet in most of the cases. Especially for Mice Protein, Activity, and MNIST, our model has better accuracy by a margin of 2.5%-3.5%. On COIL-20, Lemhadri et al. preprocessed the data by resizing them to  $20 \times 20$  images. We ran our experiment on the original images. Apart from comparing with LassoNet, we also presented accuracies using all features and the optimum number of features. In most cases, the optimum number of features gave a reasonably good performance compared to all features. It's noteworthy that MNIST and COIL-20 classification using the optimum number of variables is slightly better than all; we used only 48% and 8.7% of total features, respectively. The superior performance of our model on a wide range of data sets suggests that Sparse Centroid-encoder may be applied as a feature detector in many domains.

Data set	Top 50 features		Optimum no. of features		Centers / Class	All features
	LassoNet	SCE	No. of features	SCE	for SCE	An leatures
Mice Protein	95.8	$99.10 \pm 0.51$	22	$99.46 \pm 0.44$	1	100.00
MNIST	87.3	$\textbf{90.78} \pm \textbf{0.09}$	377	$97.93 \pm 0.03$	1	$97.60 \pm 0.08$
FMNIST	80.0	$\textbf{80.27} \pm \textbf{0.11}$	355	$88.61 \pm 0.10$	3	$90.16 \pm 0.17$
ISOLET	88.5	$89.06 \pm 0.27$	245	$95.51 \pm 0.21$	5	$96.96 \pm 0.16$
COIL-20	99.1	$98.03 \pm 0.28$	90	$99.83 \pm 0.17$	1	$98.87 \pm 0.52$
Activity	84.9	$87.53 \pm 0.49$	90	$89.42 \pm 0.67$	4	$92.81 \pm 0.29$

Table 1: Classification results using LassoNet and SCE features on six publicly available data sets. We compared LassoNet with SCE using the top 50 variables, and we also reported accuracy using the optimum number and all features for each data set. Numbers for LassoNet are reported from [26]. All the reported accuracies were measured on the test set.

### 3.2.2 Single Cell Data

GM12878 is a single cell data set that has been previously used to test multiclass feature selection algorithms [20]. The samples were collected from the annotated DNA region of lymphoblastoid cell line. Each sample is represented by a 93 dimensional features sampled from three classes: active enhancer (AE), active promoter (AP) and background (BG) where each class contains 2,156 number of samples. The data set is split equally into a separate training, validation and test sets. We used the validation set to tune hyper-parameters and to pick the optimal number of features. After the feature selection step, we merged the training and validation set and trained K=10 centroid-encoder classifiers with the selected features, and reported classification accuracy on the test set.

We use the published results for deep feature selection (DFS), shallow feature selection, LASSO, and Random Forest (RF) from the work of Li et al. to evaluate SCE as shown in Table 2. To compare with Li et al., we used the top 16 features to report the mean accuracy of the test samples. We also report the test accuracy using the top 48 features picked from the validation set, this was the best result in our experiment. When restricted to the top 16, we see that the SCE features still outperform all the other models.

Models	No. of Features	Accuracy	
SCE	48	$89.40 \pm 0.24$	
SCE	16	$88.33 \pm 0.13$	
Deep DFS	16	85.67	
Shallow DFS	16	85.34	
LASSO	16	81.86	
Random Forest	16	88.21	

Table 2: Classification accuracies using the top 16 features by various techniques. Results of Deep DFS, Shallow DFS, LASSO, and Random Forest are reported from [20]. We present accuracy with the top 48 features which were selected from a validation set.

Among all the models, LASSO features exhibit the worst performance with an accuracy of 81.86%. This relatively low accuracy is not surprising, given LASSO is a linear model.

The classification performance gives a quantitative measure that doesn't reveal the biological significance of the selected genes. We did a literature survey of the top genes selected by sparse centroid-encoder and provided the detailed description in the appendix. Some of these genes play an essential role in transcriptional activation, e.g., H4K20ME1 [28], TAF1 [29], H3K27ME3 [30], etc. Gene H3K27AC [31] plays a vital role in separating active enhances from inactive ones. Besides that, many of these genes are related to the proliferation of the lymphoblastoid cancer cells, e.g., POL2 [32], NRSF/REST [33], GCN5 [34], PML [35], etc. This survey confirms the biological significance of the selected genes.

### 3.2.3 Indian Pines Hyperspectral Imagery

Here we compare SCE with sparse support vector machines on the well-known Indian Pines hyperspectral imagery of a variety of crops following the experiments in ([19]). The task is to identify the frequency bands which are essential to assign a test sample correctly to one of the sixteen classes. We took all the 220 bands in the feature selection step, including the twenty water absorption bands. Note that in literature these noisy water absorption bands are often

excluded before the experiments [36, 37]. We wanted to check whether our model was able to reject them. In fact, our model did discard them as no water absorption bands were in the top 100 features. It appeared that SSVM included some of these noisy bands as described in [19].

We followed the experimental protocol in [19]. The entire data set is split in half into a training and test set. Because of the small size of the training set, we did a 5-fold cross-validation on the training samples to tune hyper-parameters. After the feature selection on the training set, we took top n=1,2,3,4,5,10,20,40,60,80 features to build a CE classifier on the training set to predict the class labels of the test samples. For each n we repeat the classification task K=10 times. Note that we compared the performance of SCE and SSVM features without spatial smoothing for a more direct comparison of the classification rates. Figure 6 presents the accuracy on the test data using the top n bands (n=1,2,3,4,5,10,20,40,60,80) which were calculated on the training set. Classification using SCE features generally produces better accuracy. Notice that SCE features yield better classification performance using fewer bands. In particular, the accuracy of the top SCE feature (band 13) is at least 15% higher than the top SSVM feature (band 1). See the Appendix for additional details on the feature sets selected.

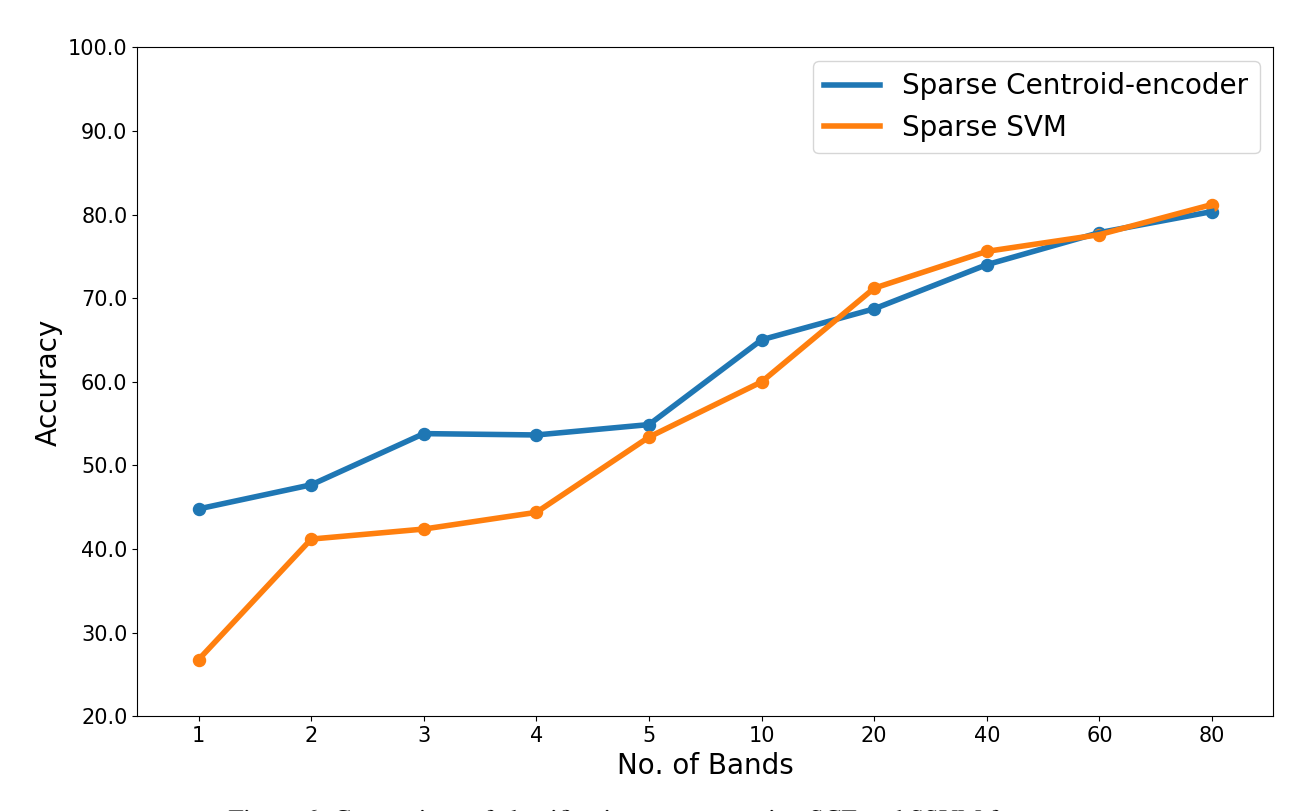


Figure 6: Comparison of classification accuracy using SCE and SSVM features.

# 3.2.4 Respiratory Infections in Humans

GSE73072 This microarray data set is a collection of gene expressions taken from human blood samples as part of multiple clinical challenge studies [38] where individuals were infected with the following respiratory viruses HRV, RSV, H1N1, and H3N2. In our experiment we excluded the RSV study. Blood samples were taken from the individuals before and after the inoculation. RMA normalization [39] is applied to the entire data set, and the LIMMA [40] is used to remove the subject-specific batch effect. Each sample is represented by 22,277 probes associated with gene expression. The data is publically available on the NCBI GeneExpression Omnibus (GEO) with identifier GSE73072.

We conducted our last experiment on the GSE73072 human respiratory infection data where the goal is to predict the classes control, shedders, and non-shedders at the very early phase of the infection, i.e., at time bin spanning hours 1-8. Controls are the pre-infection samples, whereas shedders and non-shedders are post-infection samples picked from the time bin 1-8 hr. Shedders actually disseminate virus while non-shedders do not. We considered six studies, including two H1N1 (DEE3, DEE4), two H3N2 (DEE2, DEE5), and two HRV (Duke, UVA) studies. We used 10% training samples as a validation set—the training set comprised all the studies except for the DEE5, which was kept out for

testing. We did a leave-one-subject-out (LOSO) cross-validation on the test set using the selected features from the training set. In this experiment we compared SCE with Random Forest (RF).

The results on this data set in shown in Table 3. The top 35 features of SCE produce the best Balanced Success Rate (BSR) of 90.61% on the test study DEE5. For the Random Forest model, the best result is achieved with 30 features. We also included the results with 35 biomarkers, but the BSR didn't improve. Note both the models picked a relatively small number of features, 30 and 35 out of the 22,277 genes, but SCE features outperform RF by a margin of 7%. Although RF selects features with multiple classes using a single model, it weighs a single feature by measuring the decrease of out-of-bag error. In contrast, SCE looks for a group of features while minimizing its cost. We think the multivariate approach of SCE makes it a better feature detector than RF.

Time Bin Model		No. of Features	BSR
1 – 8	SCE	35	$90.61 \pm 2.38$
1 - 6	RF	30	$83.05 \pm 2.42$
	RF	35	$82.65 \pm 2.51$

Table 3: Balanced success rate (BSR) of LOSO cross-validation on the DEE5 test set. The selected features from training set is used to predict the classes of control, shedder, and non-shedder.

### 4 Related Work

Feature selection has a long history spread across many fields, including bioinformatics, document classification, data mining, hyperspectral band selection, computer vision, etc. It's an active research area, and numerous techniques exist to accomplish the task. We describe the literature related to the embedded methods where the selection criteria are part of a model. The model can be either linear or non-linear.

#### 4.1 Feature Selection using Linear Models

Adding an  $l_1$  penalty to classification and regression methods naturally produce feature selectors. For example, least absolute shrinkage and selection operator or Lasso [18] has been used extensively for feature selection on various data sets [41, 42, 43]. Elastic net, proposed by Zou et al. [44], combined the Lasso penalty with the Ridge Regression penalty [45] to overcome some limitations of Lasso. Elastic net has been widely applied, e.g., [46, 47, 48]. Note both Lasso and Elastic net are convex in the parameter space. Support Vector Machines (SVM) [49] is a state-of-the-art model for classification, regression and feature selection. SVM-RFE is a linear feature selection model which iteratively removes the least discriminative features until a parsimonious set of predictive features are selected [50]. IFR [5], on the other hand, selects a group of discriminatory features at each iteration and eliminates them from the data set. The process repeats until the accuracy of the model starts to drop significantly. Note IFR uses Sparse SVM (SSVM), which minimizes the  $l_1$  norm of the model parameters. Lasso, Elastic Net, and SVM-based techniques are mainly applied to binary problems. These models are extended to the multi-class problem by combining multiple binary one-against-one (OAO) or one-against-all (OAA) models. [19] used 120 Sparse SVM models to select discriminative bands from the Indian Pine data set, which has 16 classes. On the other hand, Random forest [51], a decision tree-based technique, finds features from multi-class data using a single model. The model doesn't use Lasso or Elastic net penalty for feature selection. Instead, the model weighs the importance of each feature by measuring the out-of-bag error.

# 4.2 Feature Selection using Deep Neural Networks

While the linear models are fast and convex, they don't capture the non-linear relationship among the input features (unless a kernel trick is applied). Because of the shallow architecture, these models don't learn a high-level representation of input features. Moreover, there is no natural way to incorporate multi-class data in a single model. Non-linear models based on deep neural networks overcome these limitations. In this section, we will briefly discuss a handful of such models.

[52] used group Lasso [18] to impose the sparsity on a group of variables instead of a single variable. They applied the group sparsity simultaneously on the input and the hidden layers to remove features from the input data and the hidden activation. Li et al. proposed deep feature selection (DFS), which is a multilayer neural network-based feature selection technique [20]. DFS uses a one-to-one linear layer between the input and the first hidden layer. As a sparse regularization, the authors used elastic-net [44] on the variables of the one-to-one layer to induce sparsity. The standard soft-max function is used in the output layer for classification. With this setup, the network is trained in an end-to-end fashion by error backpropagation. Despite the deep architecture, its accuracy is not competitive, and experimental

results have shown that the method did not outperform the random forest (RF) method. [53] proposed a heuristics based technique to assign importance to each feature. Using the ReLU activation, [54] provided a way to measure the contribution of an input feature towards hidden activation of next layer. [55] developed an unsupervised feature selection technique based on the autoencoder architecture. Using a  $l_{2,1}$ -norm to the weights emanating from each input node, they measure the contribution of each feature while reconstructing the input. The model excavates the input features, which have a minimum contribution. [56] proposed a RBM [57, 58] based feature selection model. This algorithm runs the risk of combinatorial explosion for data set with 50K - 60K features (e.g., microarray gene expression data set).

## 5 Discussion and Conclusion

In this paper, we presented Sparse Centroid-Encoder as an effective feature selection tool for multiclass classification problems. The benchmarking results span nine diverse data sets and six methods providing evidence that the features of SCE produce better generalization performance compared to other models. We compared SCE with deep feature selection (deep DFS), a deep neural network-based model, and found that the features of SCE significantly improved the classification rate on test data. The survey of the known functionality of these genes indicates plausible biological significance. In addition to extracting the most robust features, the model shows the ability to discard irrelevant features. E.g., on the Indian Pines hyperspectral image data set, our model didn't pick any of the water absorption bands considered to be noisy. We also compare our model to multi-class extensions sparse binary classifiers. Chepushtanova et al. used 120 binary class SSVM models on the Indian Pine data set. Similarly, Lasso needed three models for the GM12878 data. These models will suffer a combinatorial explosion when the number of classes increases. In contrast, SCE uses a single model to extract features from a multi-class data set.

SCE compares favorably to the neural network-based models deep DFS, LassoNet, where samples are mapped to class labels. SCE employs multiple centroids to capture the variability within a class, improving the prediction rate of unknown test samples. In particular, the prediction rate on the ISOLET improved significantly from one centroid to multiple centroids suggesting the speech classes are multi-modal. The two-dimensional PCA of ISOLET classes further confirms the multi-modality of the classes. We also observed an enhanced classification rate on FMNIST and Activity data with multiple centroids. In contrast, single-center per class performed better for other data sets (e.g., COIL-20, Mice Protein, GM12878, etc.). Hence, apart from producing an improved prediction rate using features that capture intra-class variance, our model can provide extra information about whether the data is unimodal or multi-modal. This aspect of sparse centroid-encoder distinguishes it from the LassoNet and DFS, which do not model the multi-modal nature of the data.

We also presented a feature selection workflow to determine the optimal number of robust features. Our experimental results showed that the prediction rate using the optimal number of features produces the best result. These results are often very competitive compared to using all features. For example, on Mice Protein data, we got an accuracy of 99.46% using only 22 variables. On MNIST and COIL-20, our approach used only 48% and 9%, respectively, of the total feature sets and actually outperform the prediction rate of all features. On the GSE73072 data set, we got more than 90% accuracy on the holdout test set using only 35 out of 22,277 features.

### References

- [1] A C Pease, D Solas, E J Sullivan, M T Cronin, C P Holmes, and S P Fodor. Light-generated oligonucleotide arrays for rapid dna sequence analysis. *Proceedings of the National Academy of Sciences*, 91(11):5022–5026, 1994.
- [2] Dari Shalon, Stephen J Smith, and Patrick O Brown. A dna microarray system for analyzing complex dna samples using two-color fluorescent probe hybridization. *Genome research*, 6(7):639–645, 1996.
- [3] Michael L Metzker. Sequencing technologies—the next generation. Nature reviews genetics, 11(1):31, 2010.
- [4] Jason A Reuter, Damek V Spacek, and Michael P Snyder. High-throughput sequencing technologies. *Molecular cell*, 58(4):586–597, 2015.
- [5] Stephen O'Hara, Kun Wang, Richard A Slayden, Alan R Schenkel, Greg Huber, Corey S O'Hern, Mark D Shattuck, and Michael Kirby. Iterative feature removal yields highly discriminative pathways. *BMC genomics*, 14(1):1–15, 2013.
- [6] Cosmin Lazar, Jonatan Taminau, Stijn Meganck, David Steenhoff, Alain Coletta, Colin Molter, Virginie de Schaetzen, Robin Duque, Hugues Bersini, and Ann Nowe. A survey on filter techniques for feature selection in gene expression microarray analysis. *IEEE/ACM transactions on computational biology and bioinformatics*, 9(4):1106–1119, 2012.

- [7] Isabelle Guyon and André Elisseeff. An introduction to variable and feature selection. *Journal of machine learning research*, 3(Mar):1157–1182, 2003.
- [8] Lei Yu and Huan Liu. Feature selection for high-dimensional data: A fast correlation-based filter solution. In *Proceedings of the 20th international conference on machine learning (ICML-03)*, pages 856–863, 2003.
- [9] Jorge R Vergara and Pablo A Estévez. A review of feature selection methods based on mutual information. *Neural computing and applications*, 24(1):175–186, 2014.
- [10] François Fleuret. Fast binary feature selection with conditional mutual information. *Journal of Machine learning research*, 5(9), 2004.
- [11] Naoual El Aboudi and Laila Benhlima. Review on wrapper feature selection approaches. In 2016 International Conference on Engineering & MIS (ICEMIS), pages 1–5. IEEE, 2016.
- [12] Chun-Nan Hsu, Hung-Ju Huang, and Stefan Dietrich. The annigma-wrapper approach to fast feature selection for neural nets. *IEEE Transactions on Systems, Man, and Cybernetics, Part B (Cybernetics)*, 32(2):207–212, 2002.
- [13] David E Goldberg and John Henry Holland. Genetic algorithms and machine learning. 1988.
- [14] James Kennedy and Russell Eberhart. Particle swarm optimization. In *Proceedings of ICNN'95-international conference on neural networks*, volume 4, pages 1942–1948. IEEE, 1995.
- [15] Thomas Navin Lal, Olivier Chapelle, Jason Weston, and André Elisseeff. Embedded methods. In *Feature extraction*, pages 137–165. Springer, 2006.
- [16] Tomojit Ghosh, Xiaofeng Ma, and Michael Kirby. New tools for the visualization of biological pathways. *Methods*, 132:26 33, 2018. Comparison and Visualization Methods for High-Dimensional Biological Data.
- [17] Tomojit Ghosh and Michael Kirby. Supervised dimensionality reduction and visualization using centroid-encoder, 2020.
- [18] Robert Tibshirani. Regression shrinkage and selection via the lasso. *Journal of the Royal Statistical Society: Series B (Methodological)*, 58(1):267–288, 1996.
- [19] Sofya Chepushtanova, Christopher Gittins, and Michael Kirby. Band selection in hyperspectral imagery using sparse support vector machines. In *Algorithms and Technologies for Multispectral, Hyperspectral, and Ultraspectral Imagery XX*, volume 9088, page 90881F. International Society for Optics and Photonics, 2014.
- [20] Yifeng Li, Chih-Yu Chen, and Wyeth W Wasserman. Deep feature selection: theory and application to identify enhancers and promoters. *Journal of Computational Biology*, 23(5):322–336, 2016.
- [21] James Bergstra, Olivier Breuleux, Frédéric Bastien, Pascal Lamblin, Razvan Pascanu, Guillaume Desjardins, Joseph Turian, David Warde-Farley, and Yoshua Bengio. Theano: a cpu and gpu math expression compiler. In *Proceedings of the Python for scientific computing conference (SciPy)*, volume 4, pages 1–7. Austin, TX, 2010.
- [22] M Aminian, T Ghosh, A Peterson, AL Rasmussen, S Stiverson, K Sharma, and M Kirby. Early prognosis of respiratory virus shedding in humans. *Scientific reports*, 11(1):1–15, 2021.
- [23] Stuart Lloyd. Least squares quantization in pcm. IEEE transactions on information theory, 28(2):129–137, 1982.
- [24] James MacQueen et al. Some methods for classification and analysis of multivariate observations. In *Proceedings* of the fifth Berkeley symposium on mathematical statistics and probability, volume 1, pages 281–297. Oakland, CA, USA, 1967.
- [25] Martin Fodslette Møller. A scaled conjugate gradient algorithm for fast supervised learning. *Neural networks*, 6(4):525–533, 1993.
- [26] Ismael Lemhadri, Feng Ruan, Louis Abraham, and Robert Tibshirani. Lassonet: A neural network with feature sparsity. *Journal of Machine Learning Research*, 22(127):1–29, 2021.
- [27] Muhammed Fatih Balin, Abubakar Abid, and James Zou. Concrete autoencoders: Differentiable feature selection and reconstruction. In *International conference on machine learning*, pages 444–453. PMLR, 2019.
- [28] Artem Barski, Suresh Cuddapah, Kairong Cui, Tae-Young Roh, Dustin E Schones, Zhibin Wang, Gang Wei, Iouri Chepelev, and Keji Zhao. High-resolution profiling of histone methylations in the human genome. *Cell*, 129(4):823–837, 2007.
- [29] Hui Wang, Elizabeth C Curran, Thomas R Hinds, Edith H Wang, and Ning Zheng. Crystal structure of a taf1-taf7 complex in human transcription factor iid reveals a promoter binding module. *Cell research*, 24(12):1433–1444, 2014.
- [30] Yichao Cai, Ying Zhang, Yan Ping Loh, Jia Qi Tng, Mei Chee Lim, Zhendong Cao, Anandhkumar Raju, Erez Lieberman Aiden, Shang Li, Lakshmanan Manikandan, et al. H3k27me3-rich genomic regions can function as silencers to repress gene expression via chromatin interactions. *Nature communications*, 12(1):1–22, 2021.

- [31] Menno P Creyghton, Albert W Cheng, G Grant Welstead, Tristan Kooistra, Bryce W Carey, Eveline J Steine, Jacob Hanna, Michael A Lodato, Garrett M Frampton, Phillip A Sharp, et al. Histone h3k27ac separates active from poised enhancers and predicts developmental state. *Proceedings of the National Academy of Sciences*, 107(50):21931–21936, 2010.
- [32] Kohji Yamada, Mutsumi Hayashi, Hiroko Madokoro, Hiroko Nishida, Wenlin Du, Kei Ohnuma, Michiie Sakamoto, Chikao Morimoto, and Taketo Yamada. Nuclear localization of cd26 induced by a humanized monoclonal antibody inhibits tumor cell growth by modulating of polr2a transcription. *PloS one*, 8(4):e62304, 2013.
- [33] A Kreisler, PL Strissel, R Strick, SB Neumann, U Schumacher, and CM Becker. Regulation of the nrsf/rest gene by methylation and creb affects the cellular phenotype of small-cell lung cancer. *Oncogene*, 29(43):5828–5838, 2010.
- [34] Yan-Wei Yin, Hong-Jian Jin, Wenjing Zhao, Beixue Gao, Jiangao Fang, Junmin Wei, Donna D Zhang, Jianing Zhang, and Deyu Fang. The histone acetyltransferase gcn5 expression is elevated and regulated by c-myc and e2f1 transcription factors in human colon cancer. *Gene expression*, 16(4):187, 2015.
- [35] Paolo Salomoni and Pier Paolo Pandolfi. The role of pml in tumor suppression. Cell, 108(2):165–170, 2002.
- [36] R Reshma, V Sowmya, and KP Soman. Dimensionality reduction using band selection technique for kernel based hyperspectral image classification. *Procedia Computer Science*, 93:396–402, 2016.
- [37] Xianghai Cao, Cuicui Wei, Jungong Han, and Licheng Jiao. Hyperspectral band selection using improved classification map. *IEEE geoscience and remote sensing letters*, 14(11):2147–2151, 2017.
- [38] Tzu-Yu Liu, Thomas Burke, Lawrence P Park, Christopher W Woods, Aimee K Zaas, Geoffrey S Ginsburg, and Alfred O Hero. An individualized predictor of health and disease using paired reference and target samples. *BMC bioinformatics*, 17(1):1–15, 2016.
- [39] Rafael A Irizarry, Bridget Hobbs, Francois Collin, Yasmin D Beazer-Barclay, Kristen J Antonellis, Uwe Scherf, and Terence P Speed. Exploration, normalization, and summaries of high density oligonucleotide array probe level data. *Biostatistics*, 4(2):249–264, 2003.
- [40] Matthew E Ritchie, Belinda Phipson, DI Wu, Yifang Hu, Charity W Law, Wei Shi, and Gordon K Smyth. limma powers differential expression analyses for rna-sequencing and microarray studies. *Nucleic acids research*, 43(7):e47–e47, 2015.
- [41] Valeria Fonti and Eduard Belitser. Feature selection using lasso. *VU Amsterdam Research Paper in Business Analytics*, 30:1–25, 2017.
- [42] R Muthukrishnan and R Rohini. Lasso: A feature selection technique in predictive modeling for machine learning. In 2016 IEEE international conference on advances in computer applications (ICACA), pages 18–20. IEEE, 2016.
- [43] Yongdai Kim and Jinseog Kim. Gradient lasso for feature selection. In *Proceedings of the twenty-first international conference on Machine learning*, page 60, 2004.
- [44] Hui Zou and Trevor Hastie. Regularization and variable selection via the elastic net. *Journal of the royal statistical society: series B (statistical methodology)*, 67(2):301–320, 2005.
- [45] Arthur E Hoerl and Robert W Kennard. Ridge regression: Biased estimation for nonorthogonal problems. *Technometrics*, 12(1):55–67, 1970.
- [46] Ben J Marafino, W John Boscardin, and R Adams Dudley. Efficient and sparse feature selection for biomedical text classification via the elastic net: Application to icu risk stratification from nursing notes. *Journal of biomedical informatics*, 54:114–120, 2015.
- [47] Li Shen, Sungeun Kim, Yuan Qi, Mark Inlow, Shanker Swaminathan, Kwangsik Nho, Jing Wan, Shannon L Risacher, Leslie M Shaw, John Q Trojanowski, et al. Identifying neuroimaging and proteomic biomarkers for mci and ad via the elastic net. In *International Workshop on Multimodal Brain Image Analysis*, pages 27–34. Springer, 2011.
- [48] Artem Sokolov, Daniel E Carlin, Evan O Paull, Robert Baertsch, and Joshua M Stuart. Pathway-based genomics prediction using generalized elastic net. *PLoS computational biology*, 12(3):e1004790, 2016.
- [49] Corinna Cortes and Vladimir Vapnik. Support vector machine. Machine learning, 20(3):273–297, 1995.
- [50] Isabelle Guyon, Jason Weston, Stephen Barnhill, and Vladimir Vapnik. Gene selection for cancer classification using support vector machines. *Machine learning*, 46(1):389–422, 2002.
- [51] Leo Breiman. Random forests. *Machine learning*, 45(1):5–32, 2001.
- [52] Simone Scardapane, Danilo Comminiello, Amir Hussain, and Aurelio Uncini. Group sparse regularization for deep neural networks. *Neurocomputing*, 241:81–89, 2017.

- [53] Seong Gon Kim, Nawanol Theera-Ampornpunt, Chih-Hao Fang, Mrudul Harwani, Ananth Grama, and Somali Chaterji. Opening up the blackbox: an interpretable deep neural network-based classifier for cell-type specific enhancer predictions. *BMC systems biology*, 10(2):243–258, 2016.
- [54] Debaditya Roy, K Sri Rama Murty, and C Krishna Mohan. Feature selection using deep neural networks. In 2015 International Joint Conference on Neural Networks (IJCNN), pages 1–6. IEEE, 2015.
- [55] Kai Han, Yunhe Wang, Chao Zhang, Chao Li, and Chao Xu. Autoencoder inspired unsupervised feature selection. In 2018 IEEE International Conference on Acoustics, Speech and Signal Processing (ICASSP), pages 2941–2945. IEEE, 2018.
- [56] Aboozar Taherkhani, Georgina Cosma, and T Martin McGinnity. Deep-fs: A feature selection algorithm for deep boltzmann machines. *Neurocomputing*, 322:22–37, 2018.
- [57] Geoffrey E. Hinton, Simon Osindero, and Yee-Whye Teh. A fast learning algorithm for deep belief nets. *Neural Comput.*, 18(7):1527–1554, July 2006.
- [58] Geoffrey E Hinton and Ruslan R Salakhutdinov. Reducing the dimensionality of data with neural networks. *science*, 313(5786):504–507, 2006.